Title	Fabrication of skin layer on aluminum foam surface by friction stir incremental forming and its mechanical properties
Author(s)	Matsumoto, Ryo; Tsuruoka, Hiroyuki; Otsu, Masaaki et al.
Citation	Journal of Materials Processing Technology. 2015, 218, p. 23-31
Version Type	AM
URL	https://hdl.handle.net/11094/93998
rights	© 2015. This manuscript version is made available under the CC-BY-NC-ND 4.0 license https://creativecommons.org/licenses/by-nc-nd/4.0/
Note	

Title:

Fabrication of Skin Layer on Aluminum Foam Surface by Friction Stir Incremental Forming and its Mechanical Properties

Authors:
Ryo Matsumoto[1,*], Hiroyuki Tsuruoka[1], Masaaki Otsu[2] and Hiroshi Utsunomiya[1]

* Corresponding author (R. Matsumoto, E-mail: ryo@mat.eng.osaka-u.ac.jp, Tel: +81-6-6879-7500, Fax: +81-6-6879-7500)

Affiliation:
[1] Division of Materials and Manufacturing Science, Graduate School of Engineering, Osaka University, 2-1 Yamadaoka, Suita 565-0871, Japan
[2] Department of Mechanical Engineering, Faculty of Engineering, University of Fukui, 3-9-1 Bunkyo, Fukui 910-8507, Japan

Abstract

Porous metals with a nonporous skin surface layer (sandwich structure) have a potential to improve their mechanical properties. Friction stir incremental forming process for sheet metals is applied to form the surface of a closed-cell type aluminum foam. In this process, the cell walls near the aluminum foam surface are plastically deformed and stirred by the rotation of a forming tool at a very high rate, and the nonporous skin layer is fabricated on the surface of the aluminum foam. Nonporous aluminum skin layer with a thickness less than 400 μm is fabricated at the surface without internal fracture of the aluminum foam under the following forming conditions; a tool rotation rate of 8000 rpm, a tool feed rate of 60 mm/min, and a total forming depth of 7 mm. To investigate the mechanism of formation of the skin layer, the skin layers fabricated with friction stir incremental forming and incremental hammering are compared. The compressive deformation behavior of aluminum foam with a skin surface layer is investigated by performing uniaxial compression test. The specific compressive strength of aluminum foam with a nonporous skin surface layer is improved by approximately 20–60%.

Keywords: Aluminum foam; Incremental forming; Skin layer; Nonporous layer; Sandwich

component; Compressive strength

1. Introduction

Lightweight structural components are in demand in automotive industries because of environmental concerns (Kleiner et al., 2003). Since porous metals contain many pores, their density is much lower than that of nonporous metals. Owing to this, porous metals are attractive materials for weight reduction of the structural components. Banhart (2001) and Ashby et al. (2000) have previously discussed the manufacture, characterization and application of porous metals ~~have previously been discussed~~. Their porous structures are not only light in weight but also have some unique characteristics such as high energy absorbing capacity, high sound absorbing capacity and low thermal properties.

Various methods for the fabrication of porous metals have been developed. For example, Baumgärtner et al. (2000) have developed the precursor method and Miyoshi et al. (2000) have developed the casting process of molten aluminum and stabilizing bubbles for the fabrication of aluminum foam. Such porous metals must have the required characteristics if they are to be used widely in industrial products. In particular, the strength–mass relation of porous metals should be improved because the use of porous metals in structural components tends to reduce their strength as well as their mass. The control of the pore distributions of porous metals is crucial to the production of structural components with the desired characteristics, such as functionally graded properties and an enhanced strength–mass relation. In a case of forming of honeycomb sandwich panels, porous metals with a thin nonporous skin surface layer have attractive features, such as enhanced strength, an extension of the plateau region in compression (Banhart and Baumeister, 1998), a reduction in the notch effect, and simplified joining with other components. As surface treatments for enhancing the strength–mass relations of porous metals, Seeliger (2002) has suggested the fabrication of an

aluminum foam sandwich (AFS) component and Kitazono et al. (2009) have suggested the fabrication of an aluminum foam coated with resin. Alternately, metal forming processes have been used to fabricate skin layers on porous metal surfaces. For example, Lobos et al. (2009) and Koriyama et al. (2012) have applied wire-brushing and shot peening processes to form the surfaces of lotus-type porous copper for the purpose of improving their mechanical properties, respectively. In these processes, the cell walls near the surface were plastically deformed, and a nonporous skin layer with fine grains was fabricated at the surface.

In this study, in order to enhance the strength–mass relation of a closed-cell type aluminum foam, friction stir incremental forming (FSIF) process for sheet metals (Otsu et al., 2009) is implemented to form the surface of the aluminum foam. The mechanism of formation of the skin layer on the aluminum foam surface is discussed by comparing the skin layers fabricated with FSIF and incremental hammering (IH). The compressive behavior of the fabricated aluminum foam with a skin surface layer is investigated with uniaxial compression testing.

2. Friction stir incremental forming for porous metal surfaces

Friction stir incremental forming process which was originally developed as novel incremental sheet metal forming method (Otsu et al., 2009) was employed in this study to fabricate nonporous skin layers on porous metal surfaces. This process combines single point incremental sheet forming with friction stir welding. A bar-shaped tool with a flat end surface with a rotation rate of 1000–10000 rpm is pushed against the sheet metal. The sheet metal is locally deformed by the rotation and movement of the tool. In this process, the sheets are heated and introduced severe plastic deformation involving dynamic recrystallization and grain refinement that arises as a result of the friction produced by the rotation of a forming tool at a very high speed. Similar forming processes can be used in the fabrication and

forming of the aluminum foam. Hangai and Utsunomiya (2009) fabricated aluminum foam from aluminum and TiH_2 powders by performing friction stir processing (FSP). Kwon et al. (2008) modified the surface structures of aluminum foam by the friction surface modification (FSM) process. Local heating of the aluminum powder and the deformation of the aluminum foam were caused by the rotation of the tool in these forming processes, but the fabrication with these approaches of nonporous skin surface layers on porous metal surfaces has not previously been reported.

The porous metal used in this study was a commercial closed-cell type aluminum foam: ALPORAS (Shinko Wire Company, Ltd., **Figure 1**) (Miyoshi et al., 2000). The ALPORAS was produced by adding calcium to increase viscosity and titanium hydride powder as a foaming agent of molten aluminum, which was mixed in a casting chamber. The foamed melt was then cooled to form solid foam. The mean relative density of the ALPORAS was $\rho = 0.1$ (mean porosity: 0.9), and the true density was assumed to be 2.7 Mg/m^3 (pure aluminum). The mean pore diameter was $\phi4$ mm, however, the scatters of the size and shape of the pores in the aluminum foam were large, as shown in Figure 1. The ALPORAS specimen had a rectangular parallelepiped with the dimensions 30 mm x 22 mm x 24 mm.

The friction stir incremental forming process for porous metals is illustrated in **Figure 2**. Forming was carried out on a 3-axis NC milling machine. A bar-shaped tool with a flat end and a diameter of $\phi6$ mm (diameter at end surface: $\phi4$ mm) was made of high speed tool steel (JIS: SKH51, 58 HRC). The diameter at the end surface of the tool was the same as the mean pore diameter of the aluminum foam. The surface roughness at the end surface of the tool was $Ra < 1.6$ µm. The tool was pushed against the surface of the aluminum foam with a rotation rate of $\omega = 400–15000$ rpm in the z direction with $p_z = 0.5$ mm under dry condition (without lubrication). The tool pass is shown in Figure 2(c) in the x-y plane at the i-th pass number in the z direction. The tool was moved with a feed rate of $f = 20–2000$ mm/min in the

y direction and a pitch of $p_x = 0.5$ mm. The pass number in the z direction was $n = 1$–20 (total forming depth $np_z = 0.5$–10 mm). The forming conditions are summarized in **Table 1**.
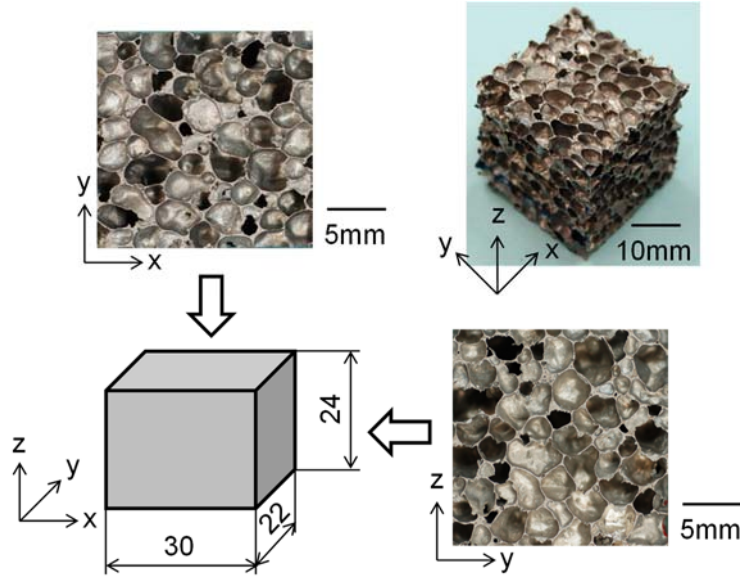

Fig. 1 Initial shape and appearance of ALPORAS specimen (mean relative density ρ: 0.1, mean pore diameter: $\phi 4$ mm).
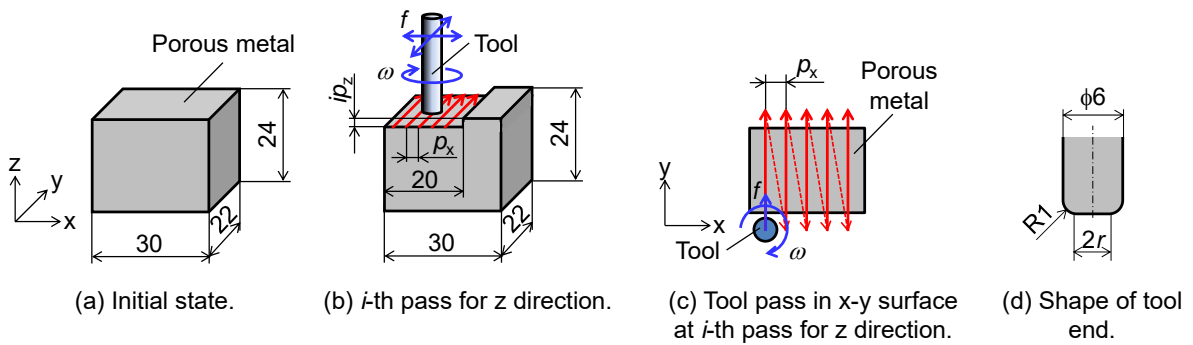

(a) Initial state.　(b) i-th pass for z direction.　(c) Tool pass in x-y surface at i-th pass for z direction.　(d) Shape of tool end.

Fig. 2 Friction stir incremental forming (FSIF) process for porous metal (ω: tool rotation rate, f: tool feed rate, p_x: forming pitch in x direction, p_z: forming pitch in z direction, i: pass number in z direction, r: radius of end surface of rotating tool).

Table 1 Friction stir incremental forming (FSIF) conditions for aluminum foam.

Tool rotation rate ω /rpm	400–15000
Tool feed rate f /mm·min^{-1}	20–2000
Moving pitch of tool in z direction p_z /mm	0.5
Moving pitch of tool in x direction p_x /mm	0.5
Total pass number of forming in z direction n	1–20
Total forming depth in z direction np_z /mm	0.5–10

3. Experimental results

3.1 Effects of varying pass number in z direction

Figure 3 shows photographs of the initial and formed aluminum foams. The surface of the aluminum foam was plastically deformed and stirred by the rotating tool, and the cell walls near the surface were gradually closed with increases in the pass number in the z direction. However, scratch marks were produced by the rotating tool along the forming pass direction on the formed surface for $n > 14$ ($np_z > 7.0$ mm) because the aluminum adhered to the end surface of the rotating tool during forming processes with higher total pass numbers. On the other hand, the thickness of the fabricated skin layer increased with increases in the total pass number. The fabricated skin layer was nonporous for $n < 14$ ($np_z < 7.0$ mm), whereas the cell walls were merely folded and overlapped in the lower region of the fabricated skin layer for $n = 20$ ($np_z = 10$ mm), as shown in **Figure 4**. In this case, a compact layer was fabricated in the lower region of the fabricated nonporous layer.

The relationship between the area fraction of the metal matrix at the formed surface (the surface area of the metal matrix/the nominal surface area of the aluminum foam) and the total forming depth in the z direction is shown in **Figure 5**. The surface whose asperity height was lower than 100 μm was defined as the metal matrix surface (nonporous skin surface). The surface asperity of the fabricated surface was measured with a 3D laser coordinate measurement machine (laser spot diameter: ϕ70 μm, repeatability of displacement: 3 μm). The measurement pitch in x and y directions was 50 μm. The target area was the center region

(18 mm x 18 mm) of the formed surface of the aluminum foam, and divided nine sections (each section: 6 mm x 6 mm). The area fraction of the metal matrix was measured at each section, and mean value of the area fraction of the metal matrix was plotted in Figure 5 (error bar: standard deviation of the area fraction). Since the measurement pitch with the laser coordinate measurement machine in x and y directions (50 μm) was less than $p_x = 0.5$ mm, the measured area fraction of the metal matrix was not depended on the scanning direction of the surface asperity. The maximum area fraction of the metal matrix was obtained above 90% at $n = 14$ ($np_z = 7.0$ mm), but the area fraction of the metal matrix was lower at $n = 20$ ($np_z = 10$ mm) because of the scratch marks was produced by the rotation and movement of the tool.

Figure 6 shows the thickness of the fabricated nonporous skin layer and the total forming depth in the z direction. The y-z cross-section of the fabricated skin layer was observed by a digital optical microscope. The thickness of the fabricated skin layer was measured for every 1 mm in y direction at 18 places, and mean thickness was plotted in Figure 6. Since scattering of pore distribution of the aluminum foam was considerably large, uniform thickness of the fabricated skin layer was not obtained. The standard deviation of the thickness of the fabricated skin layer was 150–290 μm. A nonporous skin layer with a thickness of approximately 400 μm was fabricated on the surface without internal fracture of the aluminum foam at $n = 14$ ($np_z = 7.0$ mm). This fabricated nonporous skin layer was thinner than the ideal thickness ($np_z\rho$) for forming at $n < 14$ ($np_z < 7.0$ mm) because the aluminum foam was shaved by the rotation of the tool, and the total volume of the formed region was reduced. In contrast, a thick layer was obtained at $n = 20$ ($np_z = 10$ mm), however a compact layer was observed in the lower region of the fabricated skin layer, as shown in Figure 4. Thus the tool rotation is only found to be effective in stirring the cell walls near the surface of the formed material. The maximum thickness of the fabricated nonporous skin layer is found to be approximately 400 μm under these forming conditions.
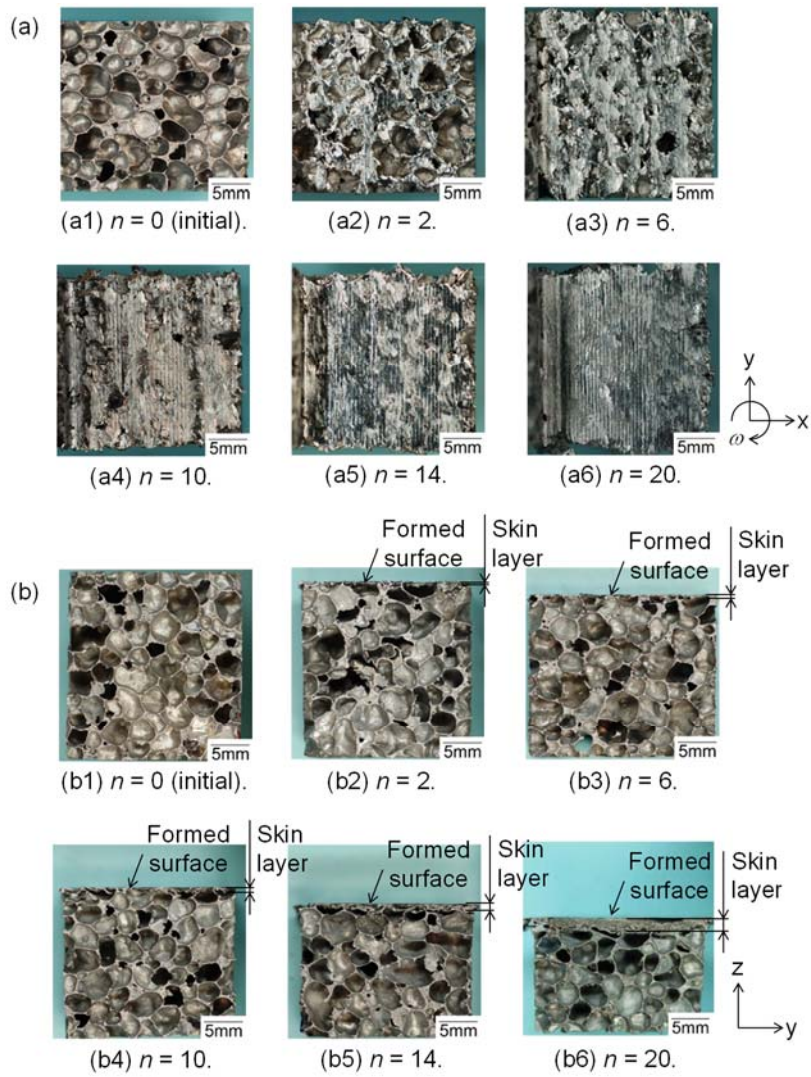
Fig. 3 Photographs of initial and formed aluminum foams (*n*: total pass number in z direction): (a) x-y surface, (b) y-z cross-section.
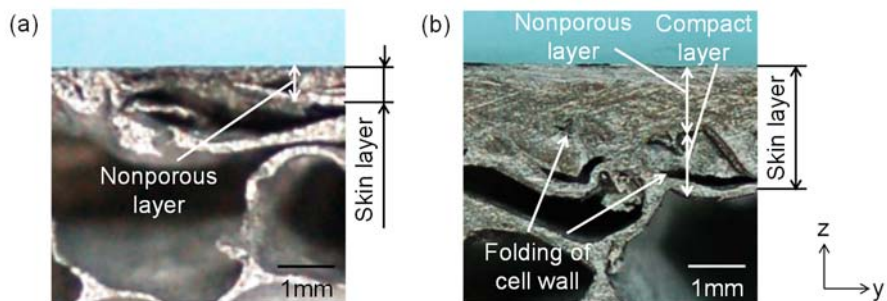

Fig. 4 y-z cross-sectional photographs of skin layer of formed aluminum foams: (a) *n* = 14, (b) *n* = 20.
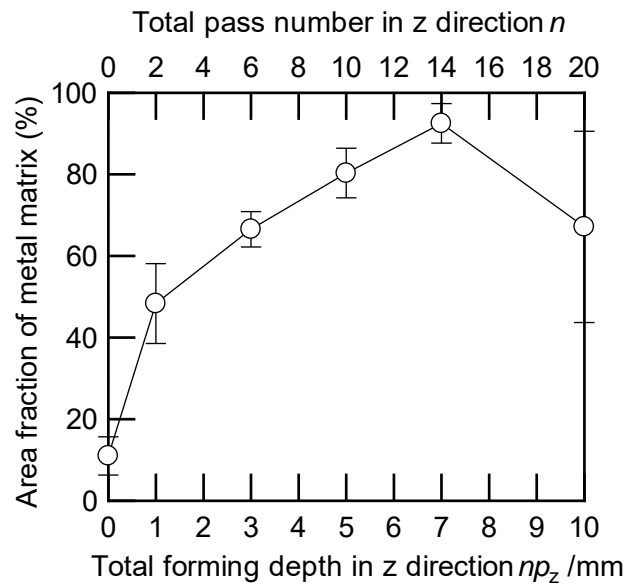
Fig. 5 Relationship between area fraction of metal matrix on x-y surface of aluminum foam and total forming depth in z direction in FSIF.
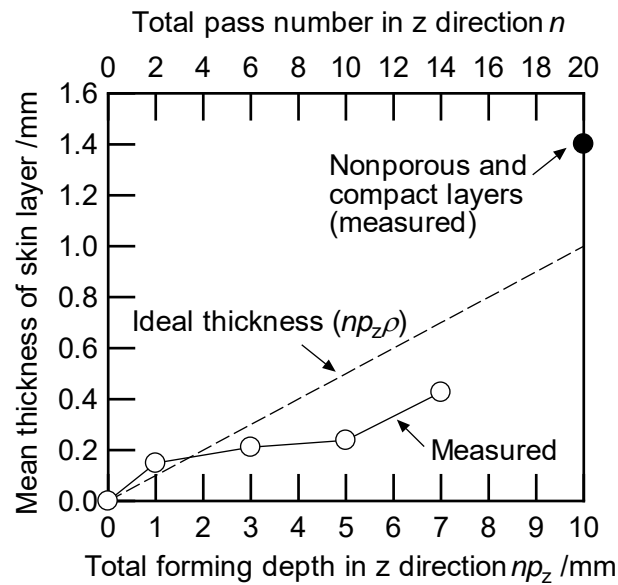

Fig. 6 Relationship between thickness of fabricated nonporous skin layer on formed aluminum foam and total forming depth in z direction in FSIF.

3.2 Effects of varying tool feed and rotation rates

Figure 7 shows the effects of varying the tool feed and rotation rates on the area

fraction of the metal matrix of the formed aluminum foam on the x-y surface at $n = 10$ ($np_z = 5$ mm). Irrespective of the tool feed rate, the area fraction increased with increases in the tool rotation rate in the range $\omega < 8000$ rpm. A skin surface with an area fraction of approximately 80% was fabricated under the forming conditions of $\omega = 8000$ rpm and $f = 60$ mm/min, but the area fraction of the fabricated skin surface was not further enhanced for $\omega > 8000$ rpm. On the other hand, low feed rates of the tool resulted in high area fractions of the metal matrix of the formed aluminum foam. It is found that the skin surface with high area fraction of the metal matrix is fabricated under the forming conditions with high tool feed rate and low rotation rate.

The above results for variations in the tool feed and rotation rates can be summarized in terms of the relative forming rate between the tool and the specimen, which is defined as follows,

$$\text{Relative forming rate} = r\omega/f \qquad (1)$$

where r is the radius of the end surface of the rotating tool (2 mm), ω is the tool rotation rate, and f is the tool feed rate. The relative forming rate means the tool movement per one tool rotation and is employed as an index of heat input in friction stir welding (Lakshminarayanan et al., 2009). The relationship between the area fraction of the fabricated skin surface and the relative forming rate is plotted in **Figure 8**. The suitable relative forming rates for fabricating skin surface with high area fraction of the metal matrix are found to be in the range $r\omega/f = 150$–500 in forming of the aluminum foam.
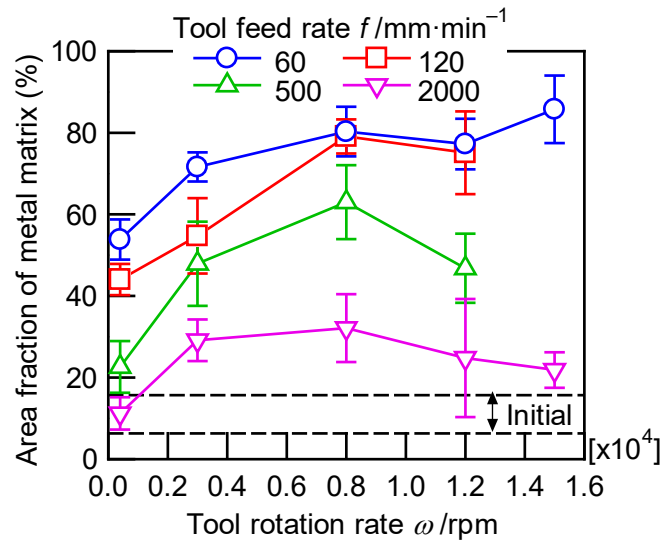
Fig. 7 Effects of varying tool feed and rotation rates on area fraction of metal matrix of formed aluminum foam on x-y surface (np_z = 5 mm).
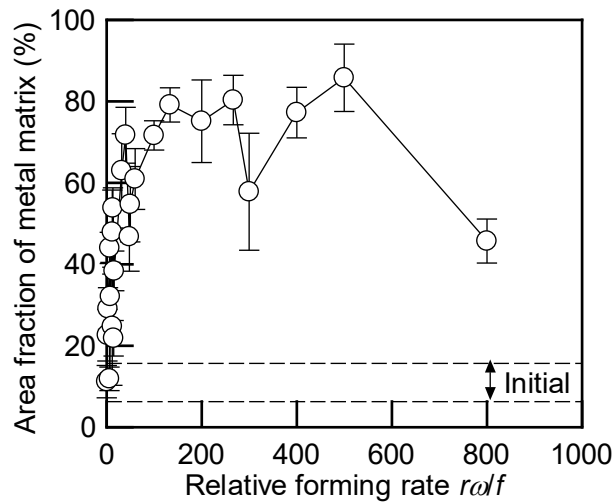

Fig. 8 Relationship between area fraction of metal matrix of formed aluminum foam on x-y surface and relative forming rate between tool and specimen (np_z = 5 mm).

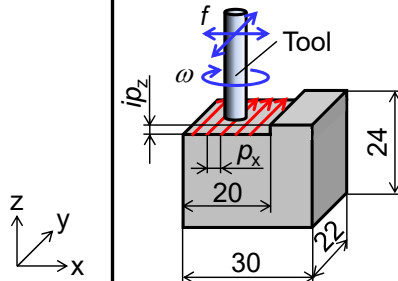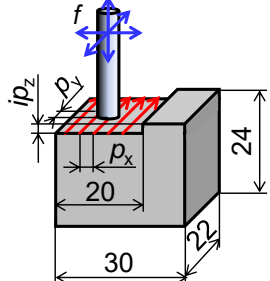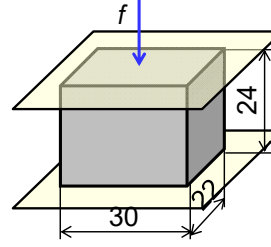## 4. Comparison with other forming methods

4.1 Forming conditions

Aluminum foam specimens formed with friction stir incremental forming (FSIF), incremental hammering (IH), and uniaxial compression were compared. The initial shape of

the aluminum foam specimen was a rectangular parallelepiped with dimensions 30 mm x 22 mm x 24 mm. The same tool was used in the implementation of the FSIF and IH methods. In the IH method, once the tool without tool rotation ($\omega = 0$ rpm) was pushed against the specimen with $p_z = 0.5$ mm, the tool was moved up for z direction. Then the tool was moved in y or x direction for $p_y = 0.5$ mm or $p_x = 0.5$ mm. After that, the tool was pushed against the specimen again. This tool pass was repeated in the x-y surface of the specimen at i-th pass for z direction. The IH specimen was incrementally hammered with the tool pass without tool rotation. The FSIF conditions were $\omega = 8000$ rpm, $f = 60$ mm/min, $p_x = p_z = 0.5$ mm, and $n = 10$, and the IH conditions were $\omega = 0$ rpm, $f = 60$ mm/min, and $p_x = p_y = p_z = 0.5$ mm (p_y: forming pitch in y direction), $n = 10$. In the uniaxial compression, the aluminum foam specimen was compressed with tungsten carbide platens with a mirror-like surface ($Ra = 0.02$–0.03 μm) under dry condition (without lubrication). The compression speed (tool feed rate) was $f = 60$ mm/min, and the compression stroke was $p_z = 5$ mm (reduction in height: 21%). The forming conditions of FSIF, IH, and uniaxial compression are summarized in **Table 2**.

Table 2 Comparison of forming conditions of friction stir incremental forming (FSIF), incremental hammering (IH), and uniaxial compression.

Forming method	Friction stir incremental forming (FSIF)	Incremental hammering (IH)	Uniaxial compression
Tool rotation rate ω /rpm	8000	0	0
Tool feed rate f /mm·min^{-1}	60	60	60 (compression speed)
Tooling pitch at i-th pass for z direction /mm	$p_x = p_z = 0.5$	$p_x = p_y = p_z = 0.5$	$p_z = 5$
Total pass number of forming in z direction n	10	10	1
Total depth of forming in z direction np_z /mm	5	5	5

4.2 Fabrication results

Figure 9 shows the aluminum foam specimens formed with FSIF, IH, and uniaxial compression for np_z = 5 mm. In the uniaxial compression specimen, cell walls were not formed near the surface and buckling of the cell wall occurred. Thus no skin layer was fabricated with uniaxial compression. Skin layers were fabricated without internal collapse or fracture on the specimens formed with the FSIF and IH methods. Furthermore, marks due to the rotating tool were observed on the formed surface of the FSIF specimen. The x-y cross-sectional photographs of the skin layer formed with the FSIF and IH methods in a position with depth of 0.1 mm from the formed surface are shown in **Figure 10**. Since the boundary of the cell walls was not observed in the nonporous layer of the FSIF specimen, the cell walls were considered to be partly joined at the surface by tool rotation process. In contrast, the cell walls were merely folded and overlapped in the IH specimen because the

boundaries of the cell walls are clearly observed in the surface (Figure 9) and the inside (Figure 10) of the skin layer. The area fractions of the metal matrix of the fabricated surface and the mean thicknesses of the skin layers fabricated with the FSIF, IH, and uniaxial compression methods are shown in **Figure 11**. The fabricated skin surface and layer in the FSIF specimen were approximately 80% of the area fraction and 240 μm in thickness, whereas the fabricated skin surface and layer in the IH specimen were approximately 65% of the area fraction and 880 μm in thickness, respectively. Here, the fabricated skin layers in the FSIF and IH specimens were the nonporous and compact (folded region of the cell walls) layers, respectively. As mentioned above, the cell walls in the fabricated skin layer in the IH specimen were not joined.
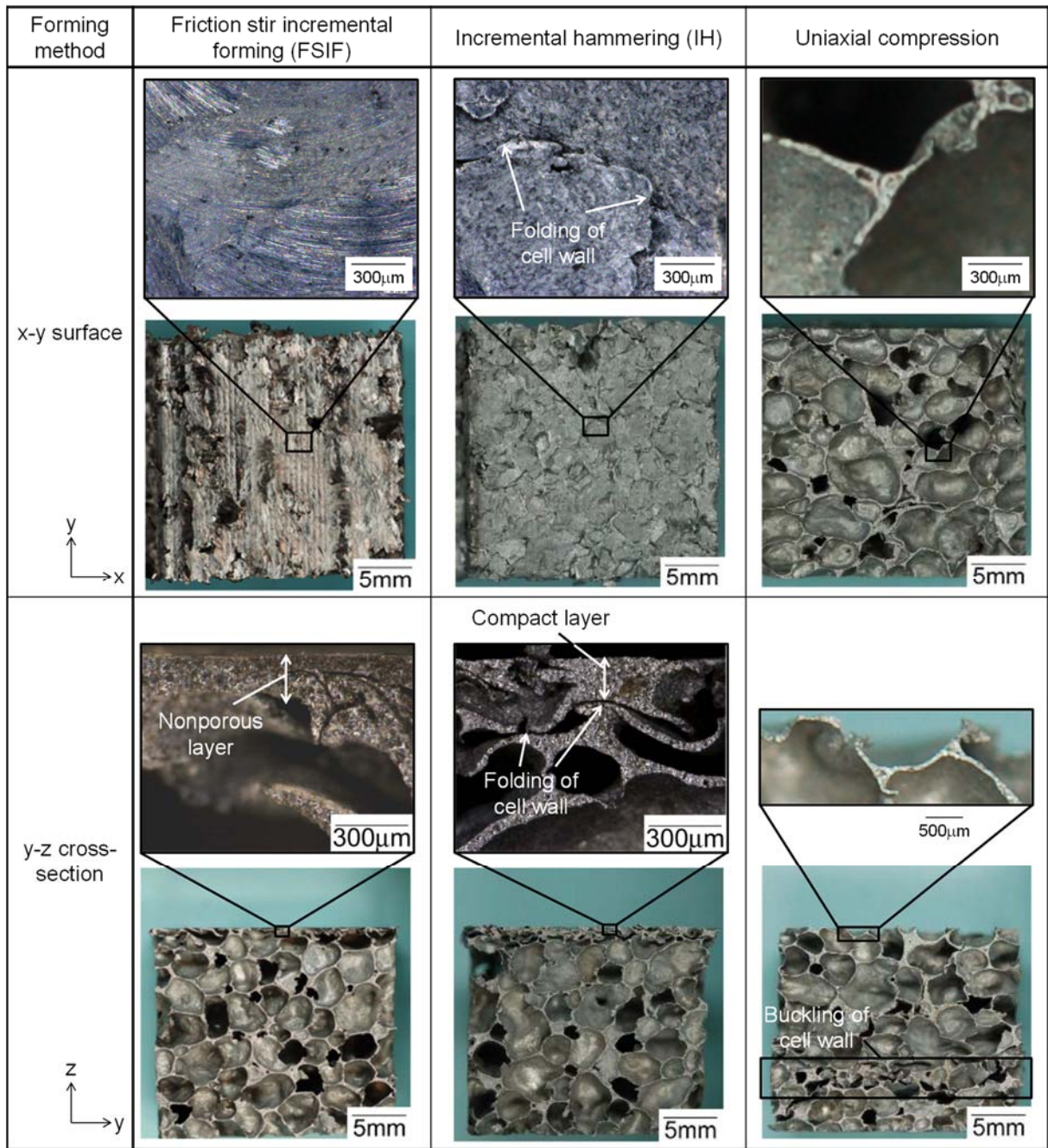
Fig. 9 Photographs of aluminum foam specimens formed with FSIF, IH, and uniaxial compression methods (np_z = 5 mm).
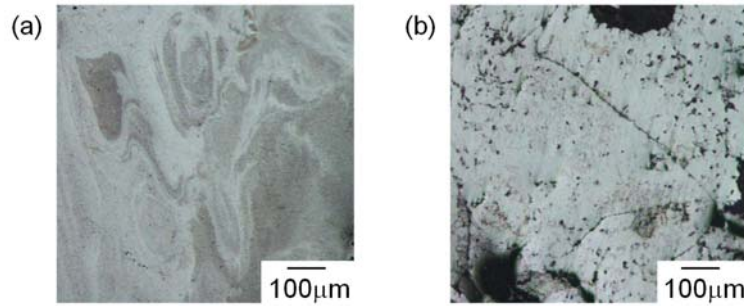
Fig. 10 x-y cross-sectional photographs of skin layer of formed aluminum foams in a position with depth of 0.1 mm from formed surface (np_z = 5 mm): (a) FSIF, (b) IH.
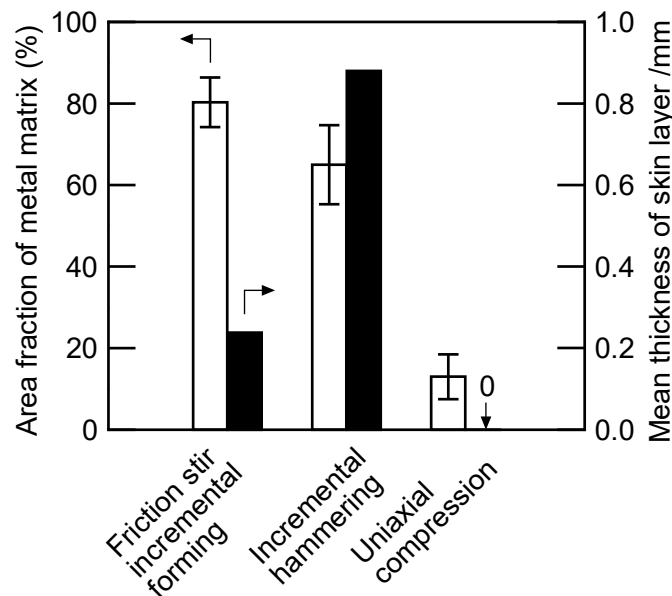

Fig. 11 Area fractions of metal matrix of fabricated surface and mean thicknesses of fabricated layers of formed aluminum foam in FSIF, IH, and uniaxial compression specimens (np_z = 5 mm).

5. Uniaxial compression behaviors of the fabricated porous metals

5.1 Compression conditions

To examine the mechanical properties of the aluminum foam specimens with skin surface layers, uniaxial compression tests were carried out. The specimens for the uniaxial compression tests were prepared with FSIF or IH method. FSIF was carried out on two or

four surfaces of the specimen under the forming conditions $\omega = 8000$ rpm, $f = 60$ mm/min, p_x = p_z = 0.5 mm, and n = 10, whereas IH was conducted on two or four surfaces of the specimen under the forming conditions $\omega = 0$ rpm, $f = 60$ mm/min, $p_x = p_y = p_z = 0.5$ mm, and $n = 10$. The resulting FSIF and IH specimens were cubes with dimensions 25 mm x 25 mm x 25 mm. **Figure 12** shows the specimens used in the uniaxial compression tests, which are as follows,

· Specimen (a): aluminum foam without a skin surface (as-received aluminum foam)

· Specimen (b1): aluminum foam with two skin surfaces fabricated with FSIF

· Specimen (b2): aluminum foam with four skin surfaces fabricated with FSIF

· Specimen (c): aluminum foam with four skin surfaces fabricated with IH

   In the uniaxial compression tests, the specimens were compressed with tungsten carbide platens with a mirror-like surface ($Ra = 0.02–0.03$ μm) under dry condition (without lubrication) on a material testing machine. The compression direction was parallel to the fabricated skin surface of the specimen, the compression speed was 2.5 mm·min^{-1}; the initial strain rate was 1.6×10^{-3} s^{-1}, and compression was performed at room temperature.
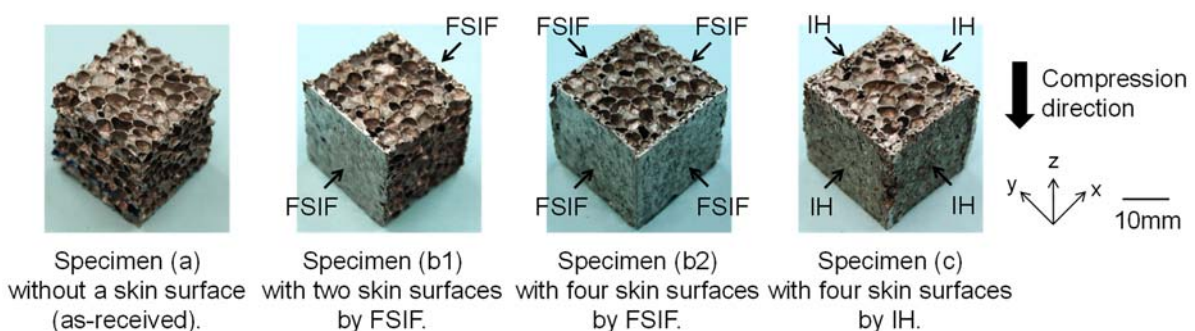

Fig. 12 Appearances of aluminum foam specimens with/without skin surfaces prior to uniaxial compression testing (FSIF: friction stir incremental forming, IH: incremental hammering).

5.2 Compression results

Figure 13 shows the appearances of the aluminum foam specimens (a), (b2), and (c) during uniaxial compression testing. As mentioned in section 4.2, buckling of the cell wall occurred in specimen (a). At a nominal compressive strain of 0.1, cracks did not appear in the surface of specimen (b2) because the cell walls in the fabricated nonporous skin layer were joined by the FSIF process, whereas cracks were observed in the surface of specimen (c) because the cell walls in the fabricated skin layer of the IH specimen were merely folded and overlapped (not joined). At a nominal compressive strain of 0.6, the fabricated skin layers of specimens (b2) and (c) were collapsed.

Figure 14 shows (i) nominal compressive stress–strain and (ii) specific nominal compressive stress–strain curves obtained in the uniaxial compression tests of the aluminum foam specimens with/without skin surfaces. The each five specimens of (a), (b2), and (c) were compressed. Here, the nominal compressive stress was calculated from the compression load and the nominal initial cross-sectional area of the specimen (25 mm x 25 mm), and the nominal compressive strain was calculated from the crosshead stroke of the material testing machine and nominal initial height of the specimen (25 mm). The specific nominal compressive stress was calculated by dividing the nominal compressive stress by the bulk density of the initial specimen in order to discuss the strength–mass relations of the specimens with/without skin surfaces. The specific stress–strain curves of all of the specimens (a)–(c) exhibited the typical deformation behaviors of porous metals; an elastic deformation region in the early stage of compression, a plateau region (almost constant stress) for nominal compressive strains in the range 0.1–0.5, and a densification region at nominal compressive strains above 0.5. In the elastic deformation region, the cell walls of the specimens were bended. In the plateau region, the cell walls of the specimens were buckled and the gas pressure enclosed in the closed cells also affected to the plateau stress. In the densification

region, the cell walls of the specimens were folded and the pores were squeezed. Due to the occurrence of the buckling or brittle fracture of the fabricated nonporous skin layer, the specific compressive stresses of specimens (b1) and (b2) were waved in the plateau region. The specific compressive stresses of specimens (b1), (b2), and (c) were improved in the range of nominal compressive strain 0.1–0.5, in particular, the specific compressive stress of specimens (b2) was approximately 1.2–1.6 times higher than that of specimen (a). The plateau region of specimens (b1), (b2), and (c) was approximately 1.2–1.4 times wider than that of specimen (a). However the specific compressive stresses of specimens (b1), (b2), and (c) for nominal compressive strain above 0.5 were lower than that of specimen (a). This difference arises because of the buckling or brittle fracture of the fabricated skin layers in specimens (b1), (b2), and (c), which means that the compressive strength dropped to the same level as that of specimen (a). In addition, the specific stresses of specimens (b1), (b2), and (c) were divided by their high bulk density. The above results confirm that the fabrication on aluminum foam of a nonporous skin surface layer fabricated with FSIF improves its specific strength.

It is known that the strengths and relative densities of porous metals are not in direct proportion (Gibson and Ashby, 1997). Thus, we analyze the improvement in the specific strength in terms of the unit cell model (Gibson and Ashby, 1997). The maximum compressive stress (σ_y) of the closed-cell unit model can be calculated as follows,

$$\sigma_y / \sigma_{ys} = 0.3(\phi\rho)^{1.5} + 0.44(1-\phi)\rho \tag{2}$$

where σ_{ys} is the yield stress of metal matrix and ϕ is the volume fraction of the metal at the cell edge. σ_{ys} and ϕ were assumed to be 130 MPa (Sugimura et al., 1997) and 0.75 (Gibson and Ashby, 1997), respectively, in this study. The values for the calculated compressive stress (σ_y) and experimentally obtained specific compressive strength as shown in Fig. 14(ii) are plotted in **Figure 15**. Since the calculated values of σ_y and the plotted experimental results for specimen (a) were in good agreement, the values of σ_{ys} and ϕ employed in eq. (2) were

reasonable. The plotted specific compressive strengths of specimens (b1), (b2), and (c) were higher than the calculated line; in particular, the specific compressive stress of specimen (b2) was 1.4 times higher than that of specimen (a). Thus, the improvement in the specific strength of the aluminum foam with a nonporous skin surface layer fabricated with FSIF is due not only to the density increase but also to the sandwich structure because it is well known that the component with sandwich structure is effective to improve its mechanical properties (Koerner, 2008). In addition, the work hardening of the nonporous skin layer during FSIF may also improve the specific strength because the skin layer was fabricated with large plastic strain by tool rotation. However, further investigation and discussion on the temperature history of the skin layer during FSIF and the microstructure observation of the skin layer are needed to clarify the phenomenon.
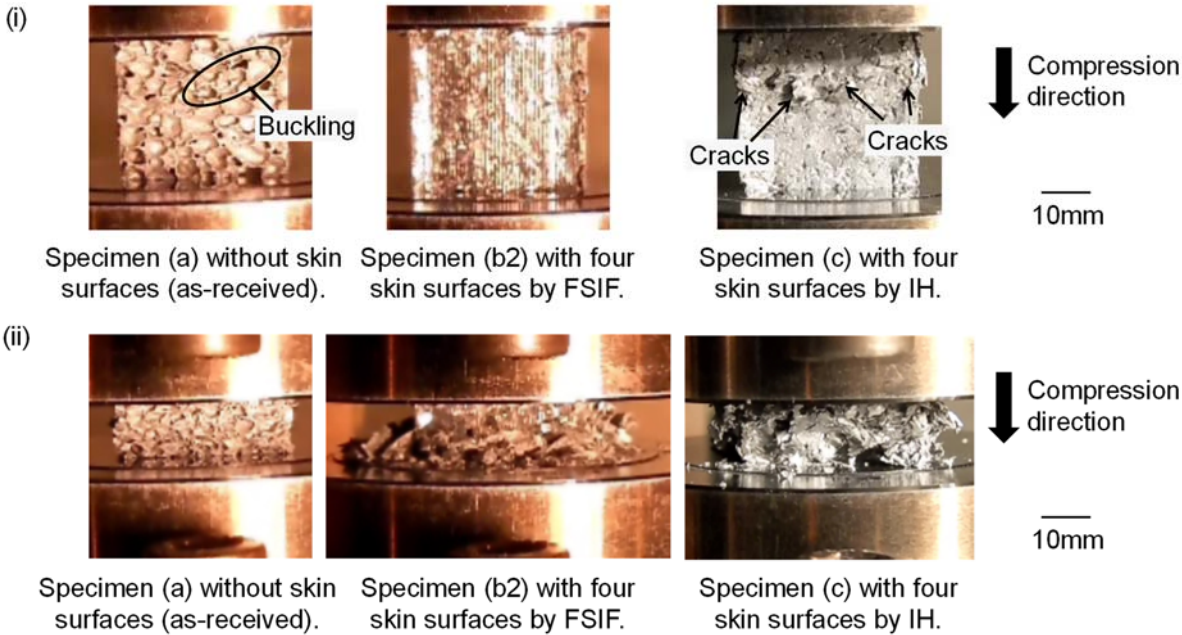

Fig. 13 Appearances of aluminum foam specimens with/without skin surfaces during uniaxial compression testing: (i) nominal compressive strain: 0.1, (ii) nominal compressive strain: 0.6.
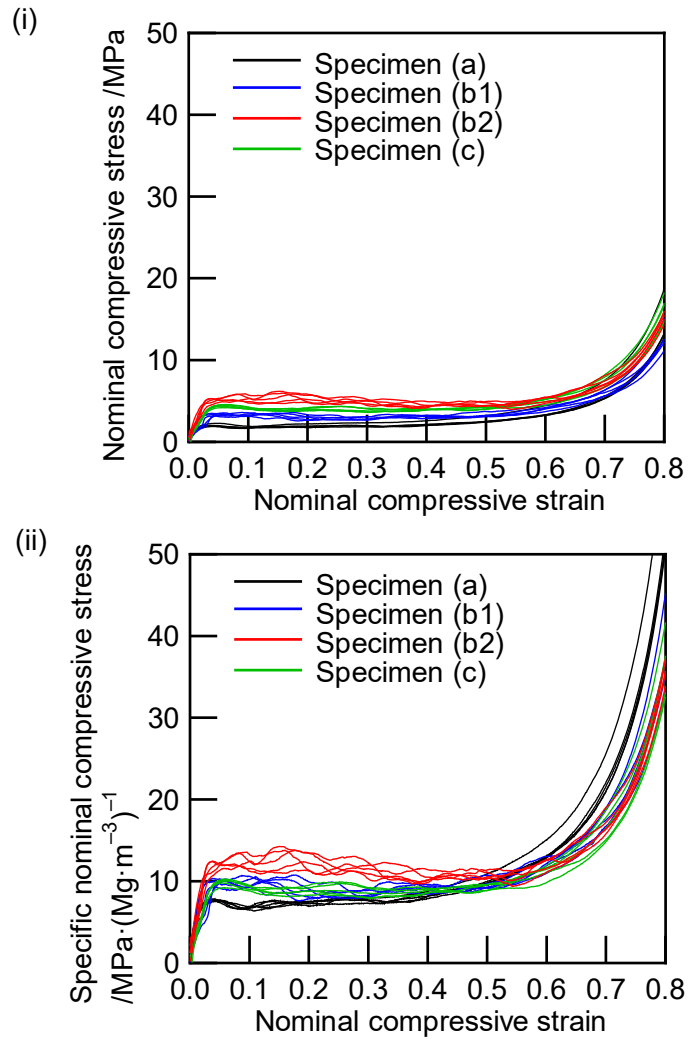
Fig. 14 Compressive deformation behaviors of aluminum foam specimens with/without skin surfaces during uniaxial compression testing: (i) nominal compressive stress, (ii) specific nominal compressive stress, (a) as-received (without a skin surface), (b1) with two skin surfaces formed with FSIF, (b2) with four skin surfaces formed with FSIF, (c) with four skin surfaces formed with IH.
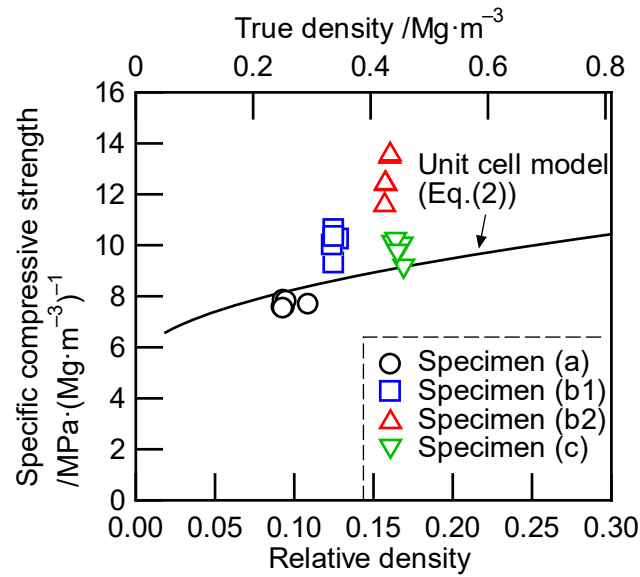
Fig. 15 Specific nominal compressive stresses of aluminum foam specimen with/without skin surfaces during uniaxial compression testing: (a) as-received (without a skin surface), (b1) with two skin surfaces formed with FSIF, (b2) with four skin surfaces formed with FSIF, (c) with four skin surfaces formed with IH.

6. Conclusions

A closed-cell type aluminum foam with a nonporous skin surface layer was fabricated with the friction stir incremental forming (FSIF) process. In this process, the cell walls near the aluminum foam surface were plastically deformed and stirred by a rotating tool with a very high rotation rate, and the nonporous skin layer was fabricated on the surface of the aluminum foam. The compressive deformation behaviors of the aluminum foam specimens with skin surface layers fabricated with the FSIF and incremental hammering (IH) methods were investigated by performing uniaxial compression test. The following conclusions were obtained.

1) A nonporous skin layer thinner than 400 μm can be fabricated on the surface of the aluminum foam without internal fracture under the following FSIF conditions; a tool rotation rate of 8000 rpm, a tool feed rate of 60 mm/min, and a total forming depth of 7

mm. The appropriate relative forming rate for the fabrication of a nonporous skin layer with a high area fraction of the metal matrix is in the range 150–500.

2) The specific compressive strength of the fabricated aluminum foam with a nonporous skin surface layer is found with uniaxial compression testing to be approximately 20–60% better than that of the aluminum foam without a skin surface layer.

3) The plateau region of the fabricated aluminum foam with a nonporous skin surface layer is found with uniaxial compression testing to be approximately 20–40% wider than that of the aluminum foam without a skin surface layer.

Acknowledgements

References

- Ashby, M.F., Evans, A., Fleck, N.A., Gibson, L.J., Hutchinson, J.W., Wadley, H.N.G., 2000, Metal Foams: A Design Guide. Butterworth-Heinemann.

- Banhart, J., 2001, Manufacture, characterization and application of cellular metals and metal foams. Progress in Materials Science. 46(6), 559-632.

- Banhart, J., Baumeister, J., 1998, Deformation characteristics of metal foams. Journal of Materials Science. 33(6), 1431-1440.

- Baumgärtner, F., Duarte, I., Banhart, J., 2000, Industrialization of powder compact foaming process. Advanced Engineering Materials. 2(4), 168-174.

- Gibson, L.J., Ashby, M.F., 1997, Cellular Solids – Structure and Properties. Cambridge University Press. 183-217.

- Hangai, Y., Utsunomiya, T., 2009, Fabrication of porous aluminum by friction stir processing. Metallurgical and Materials Transactions A. 40(2), 275-277.

- Kitazono, K., Suzuki, R., Inui, Y., 2009, Novel strengthening method of closed-cell aluminum foams through surface treatment by resin. Journal of Materials Processing Technology. 209(7), 3550-3554.

- Kleiner, M., Geiger, M., Klaus, A., 2003, Manufacturing of lightweight components by metal forming. CIRP Annals – Manufacturing Technology. 52(2), 521-542.

- Koerner, C., 2008, Integral Foam Molding of Light Metals. Springer. 45-72.

- Koriyama, S., Paiboon, S.A., Suzuki, S., Asakawa, M., Ide, T., Nakajima, H., 2012, Enhancement of the hardness of lotus-type porous copper by shot peening. Steel Research International. Special Edition, 1215-1218.

- Kwon, Y.J., Shigematsu, I., Saito, N., 2008, A novel surface modification process for porous metals using friction phenomena. Materials Letters. 62(29), 4458-4460.

- Lakshminarayanan, A.K., Balasubramanian, V., Elangovan, K., 2009, Effect of welding processes on tensile properties of AA6061 aluminium alloy joints. International Journal of Advanced Manufacturing Technology. 40(3-4), 286-296.

- Lobos, J., Suzuki, S., Nakajima, H., Ji, Y.S., Fujii, H., Terada, D., Tsuji, N., 2009, Structural change and improvement of the mechanical properties of a lotus-type porous copper by wire-brushing. Journal of Physics: Conference Series. 165, 012070.

- Miyoshi, T., Itoh, M., Akiyama, S., Kitahara, A., 2000, ALPORAS aluminum foam: production process, properties, and applications. Advanced Engineering Materials. 2(4), 179-183.

- Otsu, M., Ichikawa, T., Matsuda, M., Takashima, K., 2009, Development of friction stir incremental forming process for forming sheet metals. Proceedings of the Processing and Fabrication of Advanced Materials XVIII. 1963-1972.

- Seeliger, H.-W., 2002, Manufacture of aluminum foam sandwich (AFS) components. Advanced Engineering Materials. 4(10), 753-758.

- Sugimura, Y., Meyer, H., He, M.Y., Bart-Smith, H., Grenstedt, J., Evans, A.G., 1997, On the mechanical performance of closed cell aluminum alloy foams. Acta Materialia. 45(12), 5245-5259.